Journal of Coastal Research	18	2	338–351	West Palm Beach, Florida	Spring 2002

Geostatistical Estimation of Short-Term Changes in Beach Morphology and Sand Budget

Andrew Swales

NIWA (National Institute of Water & Atmospheric Research)
P.O. Box 11-115
Hamilton
New Zealand

ABSTRACT

SWALES, A. 2002. Geostatistical estimation of short-term changes in beach morphology and sand budget. *Journal of Coastal Research,* 18(2), 338–351. West Palm Beach (Florida), ISSN 0749-0208.

Accurate representations of beach morphology are required to address a number of research and management questions, including estimation of beach volume change. In this study, variogram modelling and ordinary kriging were used to determine short-term changes in beach morphology and sand budget, based on daily surveys of 16 beach profiles along a 500-m section of Mangawhai Beach, New Zealand. Beach elevation data were de-trended by fitting planar trend surfaces. Experimental variograms displayed a high degree of spatial continuity and there was little ambiguity involved in fitting models. Kriged beach elevations were re-combined with the trend to construct beach surfaces. Beach volume confidence intervals were derived from the trend residuals of sampled beach elevations. The difference-of-means test was used to identify statistically significant changes in beach volume from the daily profile data. On average, statistically significant changes in beach volume were detected every 5.8 days. At least 8 equally spaced profiles were required to reproduce the beach morphology to a similar level of accuracy as the complete data set. Sample location was equally important as the number of samples in minimising estimation errors. The questions of how often and how intensively to sample for monitoring beach sand resources can be answered by conducting a pilot geostatistical study and by considering the objectives of a particular study. Geostatistics provides tools to make informed decisions about beach monitoring.

ADDITIONAL INDEX WORDS: *Profiles, trend-surfaces, variograms, kriging, morphology, sand budget.*

INTRODUCTION

Beach profiles are commonly used to quantify changes in beach morphology, the assumption being that a single profile is representative of the three-dimensional (3D) morphology of a beach segment. How good this assumption is in reality largely depends on the longshore variability in the shore-normal beach profile. Beach morphology is complex due to spatial and temporal variations in wave energy, sediment supply, sediment size and composition, rhythmic topography and the occurrence of natural (*e.g.,* reefs, headlands and estuaries) and constructed (*e.g.,* groynes, jetties) features that locally influence the magnitude and direction of sand transport.

Accurate representation of beach 3D morphology is required to address a number of coastal research and management problems. In the research domain, the accuracy of numerical models of coastal processes (*e.g.,* wave shoaling and sediment transport) not only depends on the mathematical definition of the processes and boundary conditions, but also accurate representation of beach and shoreface morphology. Beach profiles are also used to validate model predictions of sand transport and consequent changes in beach state.

In the realm of coastal management, accurate sand volume estimation is required to monitor rates of beach erosion and accretion, and on developed coasts, the maintenance of a minimum beach volume is a strategy used to mitigate storm erosion and inundation hazards. Beach re-nourishment is a common 'soft' engineering approach to reconstructing eroded beaches, and the design and performance monitoring of a re-nourishment project requires very accurate sand volume estimation. In the United States, an average volume error of less than 12.2 $m^3 m^{-1}$ beach is required to satisfy the 10–20% cost contingencies associated with re-nourishment projects (GROSSKOPF and KRAUS, 1994). The coastal environment is also an important source of construction aggregates. Quantifying the size of the resource and monitoring the physical effects of sediment extraction is another application where accurate estimation is required.

In this paper spatial estimation techniques are used to model beach 3D morphology and to assess the accuracy of beach volume estimates. A critical aspect of spatial estimation is quantifying the total error, which has 2 components: measurement error and estimation error. The estimation error is the difference between an estimate and the true value at an unsampled location (ISAAKS and SRIVASTAVA, 1989). To estimate the value of a variable (*e.g.,* beach elevation) at an unsampled location, including the estimation error, involves modelling its spatial continuity. This is addressed by a branch of applied mathematics known as geostatistics (CRESSIE, 1990).

Minimising the estimation error is important if statistically significant changes in a spatial variable are to be detected and is influenced by the temporal and spatial characteristics

01130 received and accepted 19 December 2001.

of the sampling. For example, on an accreting beach it is likely that a significant change in sand volume will be measured over weeks or months because the apparent change in beach volume is large in comparison to the estimation error. However, at smaller time scales (*i.e.,* hours–days) it is more difficult to detect significant changes in sand volume because the magnitudes of the volume change and the error are similar. Also, because beach longshore shape is not uniform, the accuracy of a beach volume estimate will be determined by the location and number of samples (*e.g.,* beach profiles).

Environmental agencies charged with beach monitoring need to optimise the allocation of their often limited resources. Therefore, from a resource manager's perspective, what is an appropriate strategy to minimise data requirements for accurate modelling of beach 3D morphology? In this paper, the utility of geostatistical methods to model short-term changes in a beach sand budget are evaluated using a detailed beach profile data set from Mangawhai Beach, Northland, New Zealand.

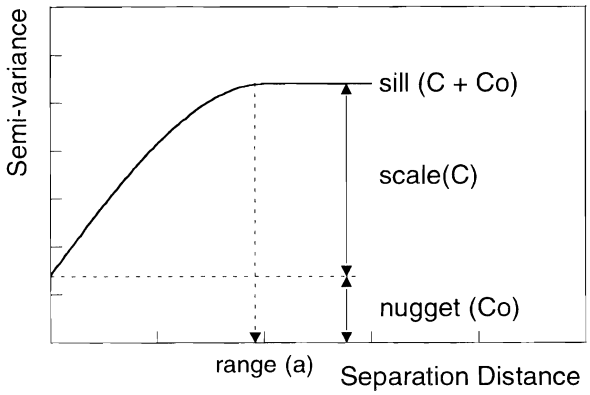

Figure 1. Example variogram. At the model range (a) the semi-variance or sill value approaches the overall sample variance. The sill may include a nugget effect (C_o), indicating a spatial discontinuity near the origin. In the absence of a nugget effect the sill is equal to the scale (C) of the variogram.

GEOSTATISTICAL ESTIMATION

Distinguishing features of geostatistical estimation include modelling the spatial continuity of a variable, using tools such as the semi-variogram (variogram), and customising the spatial estimation algorithm (*i.e.,* ordinary kriging) using the variogram model (ISAAKS and SRIVASTAVA, 1989). Geostatistical techniques were first applied in the 1950's to the problem of gold ore reserve estimation (CRESSIE, 1990). From this early applied work, geostatistical theory was developed and from it grew the spatial estimation technique known as kriging (MATHERON, 1963).

Although geostatistical methods have subsequently been applied to many areas of science where spatial estimation is required, their application to coastal research problems has only occurred in the last decade or so. In an early study, PHILLIPS (1985) used variograms to optimise the spacing of elevation measurements along beach profiles. Long-term variations in rates of shoreline accretion and erosion, including their estimation errors, have been analysed by DOLAN *et al.* (1992) using geostatistical methods. FRENCH *et al.* (1995) adopted a geostatistical approach to map spatial variations in short-term sedimentation rates in a tidal wetland. CARTER and SHANKER (1997) modelled the small-scale morphology of braided river channels to improve predictions of river hydrodynamic behaviour. To help predict the inundation of coastal lowlands by storm surges MASON *et al.* (1997) used geostatistical techniques to construct digital elevation models of a 196 km^2 intertidal flat from remotely-sensed elevation data.

The regionalised variable is a key concept in geostatistics and has properties of both a random and purely deterministic variable. Unlike truly random variables, regionalised variables (*e.g.,* beach surface elevation) display spatial continuity, however spatial variations in the value of a regionalised variable are so complex that its value at an unsampled location cannot be predicted in a purely deterministic manner (ISAAKS and SRIVASTAVA, 1989). In geostatistics, the use of a stationary random function model recognises the uncertainty in predicting the value of a spatial variable at an unsampled location. The extent to which the stationarity assumption is satisfied will determine how well geostatistical tools, such as the semi-variogram, describe the spatial continuity of a sample data set.

The Experimental Variogram

The spatial continuity of a regionalised variable is determined by sampling its value at different locations and constructing an experimental variogram. The experimental variogram approximates the 'true' spatial continuity of the phenomenon being considered. The extent to which this is achieved largely depends on how representative the sample data set is of the regionalised variable. In turn, the combination of weights assigned to nearby samples by ordinary kriging, to estimate a value at an unsampled location, depends on the model of spatial continuity fitted to the experimental variogram. Consequently the construction, interpretation and modelling of the experimental variogram are central to any geostatistical study.

If we initially assume a uniform spacing of data in a particular direction, the experimental semi-variance (γ_h), equal to half the averaged squared difference between pairs of data points (X), is calculated for increasing horizontal separation vectors or lags (h) by:

$$\gamma_h = \frac{1}{2N(h)} \sum_{i=1}^{N(h)} (X_i - X_{i+h})^2 \quad (1)$$

where N(h) is the number of comparisons between pairs of points separated by h. At lag zero, points are compared with themselves and so γ_h is zero. As the separation distance increases, the value of the regionalised variable at each location becomes less similar and γ_h increases. At some separation vector there is no longer a relationship between pairs of samples and the semi-variance approaches the value of the overall sample variance (Figure 1). The distance at which this occurs is called the range (a). The value of γ_h when the semi-variance approaches the sample variance is called the sill,

which is the total possible variation in the regionalised variable for any given h. The range defines a local neighbourhood within which sample data provide information about the value of the regionalised variable at the estimate location (DAVIS, 1986). The assumptions of the random function model become increasingly tenuous at large separation distances and in practice the maximum lag used to construct an experimental variogram is approximately half the maximum distance between samples. In some situations the semi-variance at very small lag intervals may be quite large, causing a jump or discontinuity at the origin, which is termed the nugget effect (C_o). The variogram scale (C) is equal to the sill value when the nugget effect is zero. The sill ($C + C_o$) is the total possible variation in the dependent variable and the ratio of the nugget effect to the sill value is the relative nugget effect.

In real-world situations the spacing of data is not regular and only a small proportion of the data pairs are likely to coincide with a discrete separation vector. To overcome this limitation, tolerances in the separation distance and direction are used so that while the number of lag pairs is adequate it is not so large that the pattern of the spatial continuity in a particular direction is blurred. When the angular tolerance is large (*i.e.,* 90°), an omni-directional variogram is produced, which summarises the spatial continuity of the entire data set.

Anisotropy

Directional variograms may reveal significant differences in the range and/or sill in different directions. This anisotropy in the spatial continuity of the variable is either geometric (i.e., variogram range changes), zonal (*i.e.,* variogram sill changes) or a mixture of both. The axes of anisotropy can be identified by trial and error, by mapping the two-dimensional semi-variance surface, and from knowledge of the spatial phenomenon under consideration. Qualitative information about the phenomena being studied can significantly improve the estimation. In this study, there is apparent zonal and geometric anisotropy in the beach elevation data. The apparent zonal anisotropy is a consequence of the lower variance of beach elevation in the longshore direction. The anisotropy ratio, defined by the relative ranges of the direction variograms, provides a measure of the statistical distance between samples and the estimate location. When the ratio is high, samples along the axis of maximum spatial continuity may have a larger weighting than samples that appear closer in Euclidean space.

The Model Variogram

Experimental variograms provide estimates of spatial continuity at discrete lags and in particular directions (the omni-directional variogram being an exception). However, spatial estimation at unsampled locations requires semi-variance values not coincident with the discrete lags and directions sampled by the experimental variogram(s). Therefore, to compute the statistical distance between an estimate and nearby samples, a model of spatial continuity is fitted to the experimental variogram (ISAAKS and SRIVASTAVA, 1989). Models can be fitted using some form of least squares criteria, by

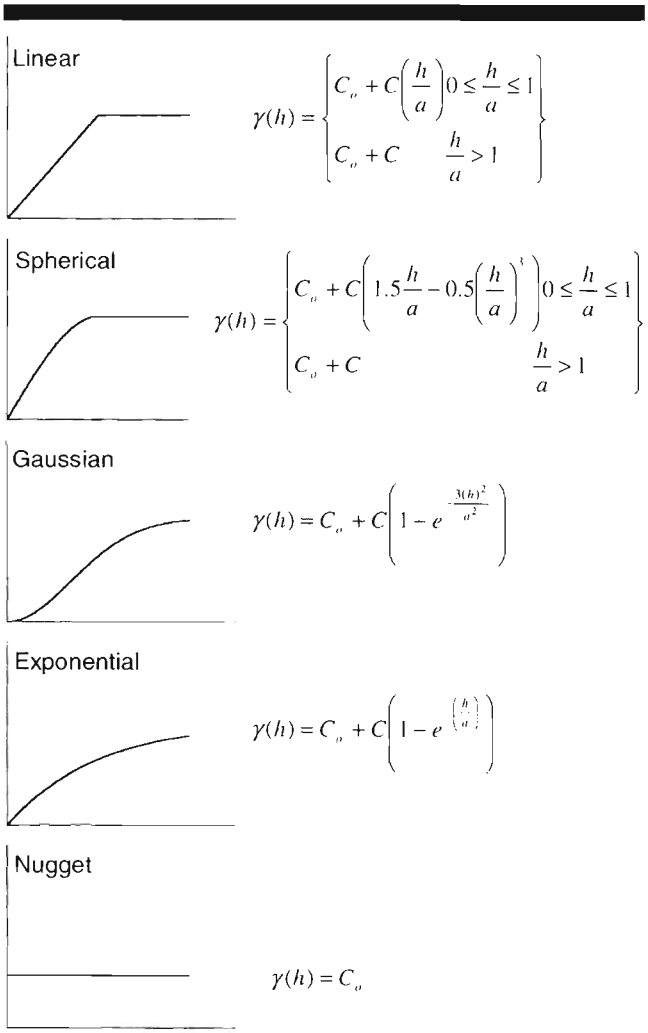

Figure 2. Variogram models commonly fitted to spatial data.

trial-and-error (*e.g.,* cross-validation), or from qualitative information about the regionalised variable (ENGLUND and SPARKS, 1991).

The variogram model must conform with several mathematical constraints, in particular the condition that a function is positive-definite. The positive-definite condition ensures a unique, stable solution to the set of simultaneous linear equations required by ordinary kriging and guarantees that individual kriging weights exceed or equal zero, sum to one and that the estimation error will have a positive variance (ISAAKS and SRIVASTAVA, 1989). There are several commonly used variogram models that are known to be positive-definite and that can be combined or 'nested' to model complex patterns of spatial continuity (Figure 2). Several basic variogram models, including the spherical, exponential and Gaussian models, incorporate a sill and range. The nugget model specifies a constant semi-variance at all lags. At small lags, the linear, spherical and exponential models have similar initial slopes, however the linear model is only positive-definite in one dimension.

In this study, nested Gaussian and spherical variogram models were found to best describe the experimental variograms of residual beach elevation. The residual elevation (Z_R) is the elevation with a trend (Z_T) removed. The spherical model is linear at small lags, with the slope sharply declining near the sill. The slope near the origin reaches the sill at two-thirds of the variogram range. The spherical model is often termed the ideal variogram shape and is analogous to the normal distribution used in statistics (CLARK, 1979). The Gaussian model is a transition model used to model extremely continuous spatial phenomena (*i.e.,* very smooth functions) and approaches the sill value asymptotically (ISAAKS and SRIVASTAVA, 1989).

The variogram model range also provides a basis for determining the relevance of nearby samples to estimation at a particular location and defines the search neighbourhood. In the presence of anisotropy, perpendicular directional variograms are used to define the size and orientation of the search ellipse.

Ordinary Kriging

Ordinary kriging is a spatial estimation technique that has certain statistically optimal properties. The goal of ordinary kriging is to produce unbiased estimates of a spatial parameter (*i.e.,* average error equal to zero) having, on average, the smallest possible error variance (*i.e.,* ordinary kriging variance), including an explicit statement of this error. The minimisation of the error variance distinguishes kriging from other spatial estimation techniques such as inverse-distance, triangulation and nearest-neighbour (ISAAKS and SRIVASTAVA, 1989).

Ordinary kriging incorporates the concept of a stationary random function, which provides a framework by which to estimate the value of the spatial variable at an unsampled location using a weighted linear combination of the available samples (*i.e.,* Σ weights = 1.0). The ordinary kriging weights are determined from the variogram model fitted to the experimental data. In the absence of a nugget effect, ordinary kriging is an exact interpolator in that the value of an estimate at a sampled location will be identical to the observation (*i.e.,* sample weighting = 1). Ordinary kriging also accounts for data clustering by reducing the weighting applied to samples in close proximity with similar values.

The ordinary kriging equations can be written in matrix notation as:

$$[C] = [w] \cdot [D] \quad (2)$$

and the weights given by

$$[w] = [C]^{-1} \cdot [D] \quad (3)$$

where [C] is a rectangular matrix containing the covariances between all sample locations and themselves, [w] is a column matrix of unknown weights, [D] is a column matrix of covariances between all sample locations and the location of the estimate and $[C]^{-1}$ is the inverse of matrix [C]. The ordinary kriging system accounts for two important aspects of spatial estimation: the statistical distance between samples and the estimate (*i.e.,* [D]) and sample clustering (*i.e.,* $[C]^{-1}$). ISAAKS and SRIVASTAVA (1989) provide a detailed discussion of the derivation of the ordinary kriging equations.

The extent to which the ordinary kriging variance is an accurate measure of the true estimation error depends on how closely the variogram model approximates the actual spatial continuity of the regionalised variable. In particular, the modelled sill value must be a good estimate of the true variance of the regionalised variable. The ordinary kriging variance is sensitive to changes in the variogram model sill (ENGLUND and SPARKS, 1991). Therefore the sample data underpinning the variogram model is of key importance. Consequently, there is some debate about the usefulness of the ordinary kriging variance as a measure of the true estimation error (DOLAN *et al.,* 1992; ISAAKS and SRIVASTAVA, 1989).

Cross-validation

Cross-validation is a tool that is used to discriminate between variogram models in the extent to which they describe the spatial continuity of a variable. In a cross-validation study, individual sample values are temporarily discarded and their value is estimated by ordinary kriging from other nearby samples. In this manner, cross-validation mimics the estimation process and quantifies the true estimation error at sampled locations. Cross-validation provides useful spatial information about the performance of a variogram model.

Sample clustering is a major limitation of any cross-validation exercise (ISAAKS and SRIVASTAVA, 1989) because the results are strictly applicable only to sampled locations. Also, sample clustering means that many nearby samples will be redundant (*i.e.,* spatial auto-correlation) and the cross-validation estimation errors will be unrealistically low. In many applications (*e.g.,* ore reservoir estimation) there is often a bias in sample locations that may lead to quite misleading conclusions being drawn from a cross-validation study. In the present study, the effect of sample clustering is partly offset by: (1) sampling across the entire cross-shore range of beach elevations at regular longshore intervals; and (2) the fact that the beach surface can be directly observed. Cross-validation is used in this study as a guide to assess the performance of variogram models fitted to the experimental data.

STUDY LOCATION

Mangawhai Beach is located on the east coast of the Northland Peninsula, New Zealand (Figure 3). The wave climate at Mangawhai is characterised by infrequent storm waves and low north-east swell (significant wave height [H_s] < 1 m). The highest waves are associated with sub-tropical cyclones (maximum wave height > 8 m). Tidal currents are weak (< 0.2 m s^{-1}), and wind-driven currents and waves drive sediment transport on the inner shelf and shoreface (HILTON, 1995).

Using WRIGHT and SHORT's (1984) classification, beach morphology at Mangawhai 'flips' between a straight beach and longshore bar and a mildly rhythmic beach and longshore bar with weak rip cell circulation. Both beach states were observed during the field experiment. During storms, sand is eroded from the beach and the longshore bar is largely destroyed, with storm sedimentation occurring as a wedge im-

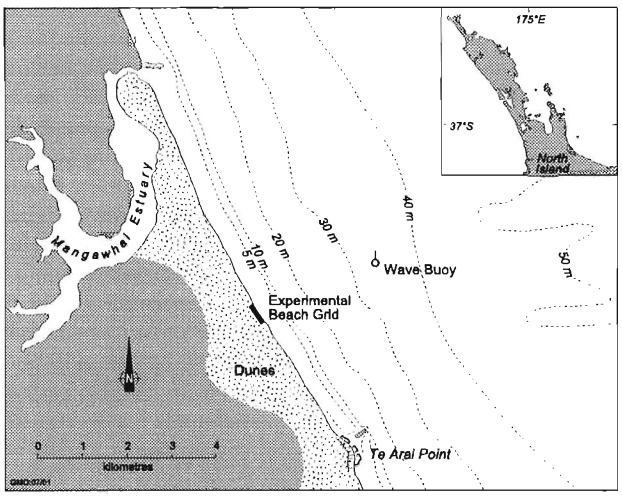

Figure 3. Location of the daily beach profile surveys at Mangawhai Beach, on the east coast of the Northland Peninsula, New Zealand.

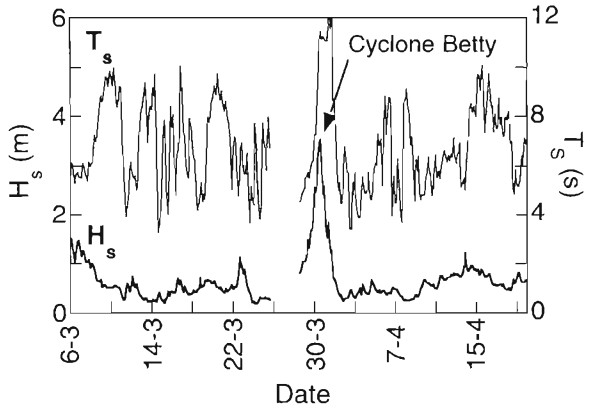

Figure 4. Significant wave height and period recorded by an ENDECO wave buoy deployed offshore from Mangawhai Beach in 35-m water depth (6 March–20 April 1996). The buoy was serviced immediately prior to Cyclone Betty.

mediately offshore from the bar. Swell waves subsequently transport sand onshore, rebuilding the beach (HICKS and GREEN, 1997; SMITH *et al.*, 1997). Beach sediments are well-sorted, fine–medium sands with median particle diameters of 0.2–0.25 mm.

The experiment was conducted within a 500-m longshore by 600-m cross-shore (to 13-m water depth) segment of the beach-shoreface during March–April 1996. The aim of the experiment was to improve knowledge of shoreface morphodynamics, including small-scale bedforms (SWALES *et al.*, 1999). As part of this work, 16 intertidal beach profiles, which were spaced at 33-m intervals alongshore, were surveyed daily. An ENDECO directional wave buoy was also deployed directly offshore in 35-m water depth. The longshore spacing of profiles was determined from analysis of earlier profile data, which showed cross-shore variograms with 30–40-m ranges. Good definition of longshore changes in beach elevation was ensured by spacing profiles at 33-m intervals. These daily beach profile data are analysed in this paper.

During the six-week experiment, Mangawhai Beach underwent a cycle of gradual beach accretion by swell waves (H_s = 0.3–1.0 m, significant wave period [T_s] = 4–10 s), rapid erosion during the Cyclone Betty storm of 30–31 March 1996 (H_s = 3.5 m, T_s = 6–13 s) and subsequent beach accretion by swell waves (H_s = 0.3–1.1 m, T_s = 3–10 s) (Figure 4).

METHODS

Beach Profile Measurements

Shore-normal beach profiles were surveyed from survey pegs located on the foredune crest using the method of EMERY (1961). Beach profile elevations were surveyed on average at 5-m intervals, to the nearest 0.01 m, by measuring elevation changes relative to the sea-horizon between two graduated 1.6-m poles. Elevations were reduced to mean sea level (MSL) using Mangawhai Trig. station 2941 (+14.98-m MSL), which is located on a dune at the northern end of the experimental area. Profile features such as berms, drainage channels, sand waves and major breaks in slope were surveyed. The beach profiles were surveyed daily between March 7–21, 23–30, April 1–3 and on April 11, 15 and 19.

Geostatistical Estimation

There are several steps to the geostatistical estimation procedure employed in this study: (1) beach grid definition; (2) de-trending daily beach elevation data; (3) modelling experimental variograms; (4) cross-validation; (5) ordinary kriging of beach elevation trend residuals; (6) combining the kriged trend residual elevations with the planar trend; (7) daily beach volume estimation; and (8) assessment of uncertainty.

Beach Grid Definition

A 100-m (cross-shore) by 500-m (longshore) beach grid was used in the geostatistical modelling. The seaward extent of profile surveys varied from day-to-day due to variations in tidal range and wave conditions. To minimise edge effects, a seaward grid boundary was selected on the basis that sampling always extended to, or beyond, the grid boundary (Figure 5). The landward boundary of the grid coincided with the foredune toe, which is approximately 4 m above MSL. In the south-west corner of the experimental grid, an outlying area of high dune (4–8 m above MSL) was excluded from the study because these elevation data degraded the de-trending procedure and the subsequent geostatistical analyses. Also, survey data showed that this area of high dune was not part of the active beach during the experiment.

The beach surface (Figure 6a) has two components: a residual (stochastic) component (Figure 6b) and an underlying trend (Figure 6c), which is mainly composed of the shore-normal beach slope. Ordinary kriging requires that the regionalised variable is stationary. De-trending enables the spatial continuity of the beach elevation data to be modelled, and used to customise the ordinary kriging algorithm.

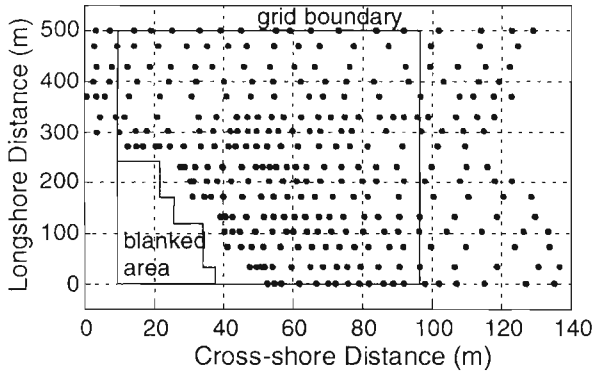

Figure 5. Beach grid with point elevation measurements for the 2 April 1996 survey. The blanked area in the south-west corner excludes an area of high dune that was not part of the active beach during the experiment.

The underlying trend in each daily beach elevation data-set was modelled by fitting a least squares planar trend surface (GOODMAN, 1983; UNWIN, 1975). Although cross-shore profiles can be approximated by non-linear functions, their greater detail was unwarranted, as the aim of the de-trending procedure is to produce stationary trend residual beach elevations. The planar trend surface equation predicts the trend component (Z_T) of the beach surface at a location (x,y) such that:

$$Z_T = b_0 + b_1(x) + b_2(y) \quad (4)$$

where b_0 is a constant, b_1 is the cross-shore (x) slope and b_2 is the longshore (y) slope.

Also, fitting a higher order trend surface (*e.g.*, quadratic) to the beach elevation data was discounted because of the inherent ill-condition of the matrix of sum of squares and cross-products [X]. Inversion of [X] is used to solve for the matrix of trend surface coefficients [b]. The matrix condition number is a measure of the relative error of the computed solution. If the trend surface coefficients [b] are known to t-digit precision and the condition number of [X] = 10^c, then the inverse $[X]^{-1}$ matrix solution may be valid to only t-c digits (CHAPRA and CANALE, 1998). The matrix inverse ($[X]^{-1}$) and condition number, for each data set, were solved using the MATLAB® software library (THE MATHWORKS INC., 1995). The matrix condition numbers were of the order 10^5–10^6, and subsequently all matrix elements were calculated at double precision (10^{14}) so that the trend surface coefficients were valid to at least eight significant figures.

To simplify subsequent geostatistical analyses and to enable direct comparison of residual elevations between surveys an average trend surface was calculated for the entire daily beach elevation data-set. The average trend relationship was further simplified by altering the constant (b_0) in equation (4) such that all residual elevations were always positive. The resulting average trend surface coefficients were $b_0 = 3$, $b_1 = -0.0333241$ and $b_2 = -0.0028218$. This average trend surface is a good approximation to the daily trend surfaces, with small variations in the cross-shore (average $b_1 \pm 1.9\%$, 95% confidence interval) and longshore (average $b_2 \pm 4.8\%$, 95% confidence interval) trend surface components.

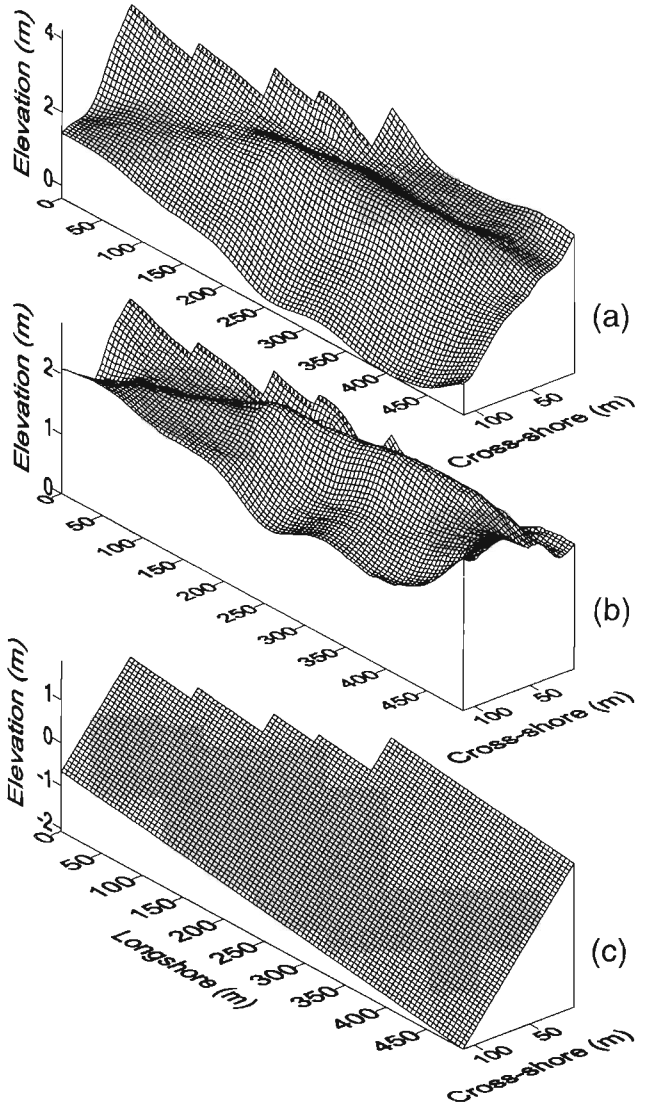

Figure 6. Three-dimensional beach surface (a) composed of (b) a stochastic elevation component and (c) an underlying planar trend.

Experimental Variograms

The geostatistical software package VARIOWIN 2.2 (PANNATIER, 1996) was used for analyses of the spatial continuity of the residual beach elevation data and variogram modelling. Spatial continuity was highest in the longshore direction and lowest in the cross-shore direction. Anisotropy axes were identified from experimental variogram surfaces, which summarise the sample semi-variance at different lags in all directions. The perpendicular anisotropy axes were found to fluctuate within narrow directional bands (±10°), orientated with the beach grid.

Geostatistical analyses applied to the residual elevation

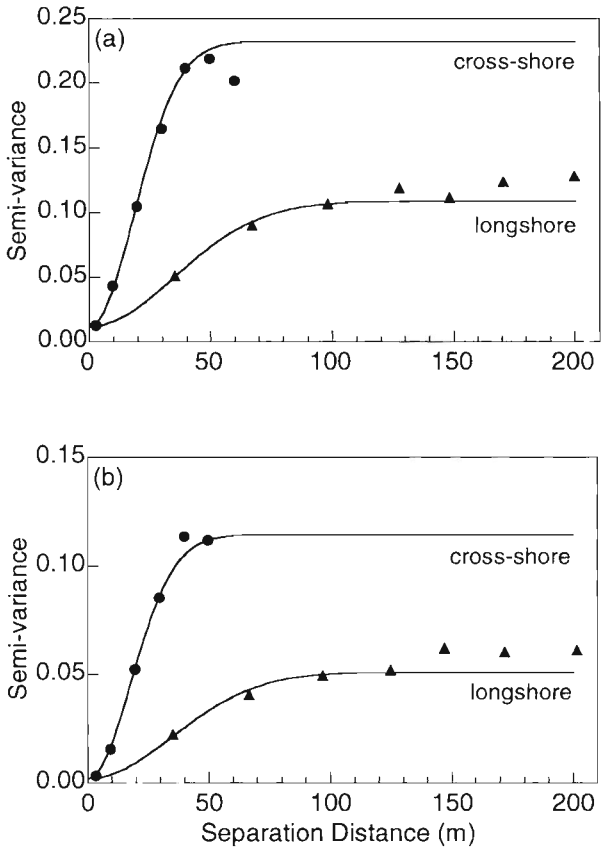

Figure 7. Gaussian variogram models, with nugget effect, fitted to the directional experimental variograms of trend residual beach elevations for (a) March 25 and (b) April 2 surveys.

data are demonstrated using pre-storm (March 25) and post-storm (April 2) examples, typical of the experimental period. Anisotropic axes for March 25 and April 2 were (5°/95°) and (10°/100°) respectively, with direction defined counter-clockwise from east (0°). By trial and error, a cross-shore lag of 7.5 m ± 3.25 m (angular tolerance ±10°) and longshore lag of 30 m ± 15 m (angular tolerance ±30°) were found to produce smooth experimental variograms. At smaller angular tolerances the experimental variograms displayed a marked 'saw-tooth' appearance as the number of data pairs fluctuated between lags.

Variogram Modelling

Variogram models were fitted to the experimental data with emphasis placed on the fit at small lags. Generally, the kriging weights reflect the statistical distance between the samples and the estimate location so that a 'good' model fit near the variogram origin is important (ENGLUND and SPARKS, 1991). The experimental variograms all displayed sills, with the sill value in the longshore direction consistently being about 50% of the cross-shore value.

Figure 7 shows the Gaussian models fitted to the March 25 and April 2 experimental variograms. At the origin, the semi-variance has a small positive value or nugget effect. The fitted nugget values for March 25 (γ_h = 0.012, 5.5% of cross-shore sill) and April 2 (γ_h = 0.002, 1.8% of cross-shore sill) are small relative to the variogram sill. The same nugget values were assumed for the longshore variograms. The larger nugget value for March 25, which indicates small-scale structure not sampled by the surveys, is consistent with the more complex beach morphology immediately prior to the storm.

The Gaussian model is less robust than the spherical model, with respect to the condition of the ordinary kriging matrices. However, the stability of the Gaussian model is much improved by the addition of a small nugget constant (*i.e.,* 1% relative nugget value) (POSA, 1988). In the present study, the fitted Gaussian models incorporate nugget constants.

The U.S. Environmental Protection Agency kriging software package GEO-EAS 1.2.1 (ENGLUND and SPARKS, 1991), which is used here for ordinary kriging of residual elevation estimates, does not implement zonal anisotropy (*i.e.,* direction dependent sill). Consequently, variogram models were nested to incorporate the sills fitted to the directional variograms. Using the April 2 data as an example (Figure 7b), the cross-shore model range is 44 m and the sill γ_h = 0.114. The cross-shore sill value is the sum of the longshore sill (*i.e.,* 0.049), the difference in directional sill values (*i.e.,* 0.063) and the nugget effect (C_0 = 0.002). The longshore variogram model requires two ranges to describe the nested structure. The first range (86 m) is derived from the model fit to the data. The second range (5000 m) is sufficiently large so that the first model structure is not altered by the second structure at distances less than the fitted range, while satisfying the requirement for a sill at γ_h = 0.114 in the cross-shore direction.

Cross-Validation

GEO-EAS was used to cross-validate the models fitted to the experimental variograms. The variogram model range(s) define the dimensions of the search ellipse and the number of nearby samples used depends on the relative nugget value. ENGLUND and SPARKS (1991) recommend using eight samples when the relative nugget value is zero and up to twenty samples when the relative nugget value exceeds 50% of the sill. In the present study, the relative nugget values average 3% (maximum 14%), so a maximum of 12 samples (minimum 6) were used to estimate residual elevations at unsampled locations. To improve estimation near the grid boundary, cross-validation included data outside the beach grid. The results of the cross-validation for the March 25 and April 2 examples are presented in the results.

Ordinary Kriging and Surfacing

GEO-EAS was used to estimate residual beach elevations and the error variance at 5100 locations on a 2-m (cross-shore) by 5-m (longshore) grid. A polygon boundary file was used to exclude the 6960 m^2 area of high dune in the southwest corner of the grid. The kriged residuals were then recombined with the average trend surface to construct the daily beach grids.

Beach Volume

Daily beach volumes above the base of the grid (−2.1-m MSL) were estimated using the SURFER® software package (GOLDEN SOFTWARE, 1995). Volumes are estimated using the trapezoidal rule, Simpson's rule and Simpson's 3/8 rule. The average volume derived from these three numerical methods was taken as the estimated beach volume. The differences in beach volumes calculated by the individual methods were always less than 0.2% of the average volume.

Beach Volume Estimation Errors

The trend residual elevations were used to estimate 95% confidence intervals (two-tailed t-test) for the daily average trend residual beach elevations. This approach is reasonable given that: (1) measurements are distributed across the entire range of beach elevations and evenly spaced alongshore so that the samples are representative of the beach surface; and (2) sample sizes are large (*i.e.,* n = 176–347) so that t is robust.

The daily beach volume estimation errors ($\pm$V m^3) were calculated as the product of the average trend residual 95% confidence intervals and the planar surface area of the beach grid (42,525 m^2). The difference of means, two-tailed, t-test was used to test the statistical significance of observed daily changes in average residual elevation during the period of gradual beach accretion from 7–30 March 1996. The null hypothesis (*i.e.,* no statistical difference in residual beach elevations at 0.05 significance level) has a rejection region where $|t| \geq 1.96$ (degrees of freedom > 120). The test was also applied to partial profile data sets to determine the effect of profile spacing and sample size on the average number of days required to detect statistical differences (*i.e.,* increases) in daily beach volumes. To determine the number of days between beach surveys required for observed changes in average residual elevations (and hence beach volume) to become statistically different, a t-matrix for all combinations of difference-of-means results was constructed. The location of a particular beach survey in the time-series is important. This is because whether or not the observed changes in average daily residual elevations are statistically different depends on the rate of change in beach volume as well as on the pooled estimation error.

Longshore Profile Spacing

The effect of altering longshore profile spacing on the accuracy of modelled beach surfaces was analysed for the March 25 and April 2 data sets. The geostatistical methods previously described were used to model beach surfaces and derive estimation errors using 16, 8, 4 and 2 beach profiles evenly spaced along the 500-m length of beach grid. The fitted trend-surfaces fell within the 95% confidence interval for the average trend surface, which was used to de-trend the data. The longshore variogram for the two profile case could not be modelled, requiring assumptions to be made about the spatial continuity of the data: a constant sill value, defined by the cross-shore variogram and a 600-m longshore range (to provide enough nearby samples). The trend residual elevations were again used to derive 95% confidence intervals for the complete and partial data sets.

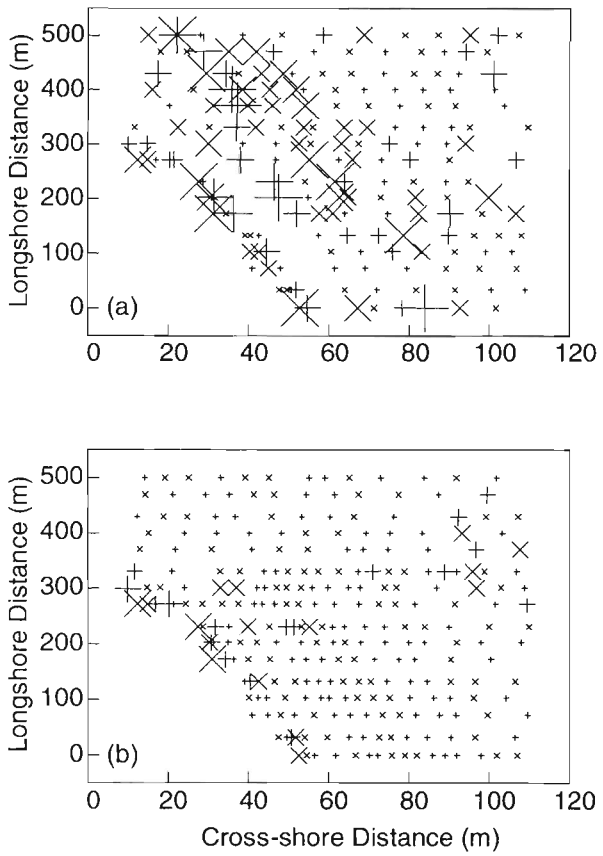

Figure 8. Spatial distribution of ordinary kriging over- (+) and under-estimation (×) of cross-validated trend residual beach elevations for the (a) March 25 and (b) April 2 surveys. For scale, the largest elevation errors were ±0.2 m.

RESULTS

Cross-validation

Cross-validation results for the example March 25 and April 2 data sets show how the fitted variogram models performed across the beach grid. While the average cross-validation errors of both data sets are negligible, the standard error of the March 25 results (±0.006 m) are three times larger than the standard error for April 2 (±0.002 m). Linear regression of the samples and estimates also shows that the April 2 variogram model (r^2 = 0.98) is a slightly better predictor of residual beach elevation than the March 25 model (r^2 = 0.94). The nugget model fitted to the March 25 data (*i.e.,* relative nugget γ_h = 5.5%) is three times larger than that fitted to the April 2 data. As a result, the cross-validation errors are larger.

The spatial distribution of under- and over-estimation is also different for both the March 25 and April 2 variogram models (Figure 8). The mapped cross-validation residuals for March 25 show that the magnitudes of under-estimates are

Table 1. *Beach elevation and volumes, 95% confidence intervals and difference of means test results for period of gradual sand accretion before Cyclone Betty.*

Survey Date	N	Elevation 95% C.I. (± m)	Volume 95% C.I. (± m³)	Difference of Means t-test No. of days to detect volume change
March 7	233	0.045	1905	1
March 8	270	0.063	2679	1
March 9	254	0.047	2011	15
March 10	219	0.044	1854	7
March 11	213	0.043	1820	5
March 12	232	0.040	1701	4
March 13	227	0.042	1786	10
March 14	222	0.046	1948	9
March 15	331	0.037	1573	8
March 16	325	0.038	1633	8
March 17	347	0.034	1425	7
March 18	214	0.044	1875	6
March 19	220	0.041	1739	5
March 20	217	0.041	1739	4
March 21	229	0.045	1909	2
March 22				no survey
March 23	194	0.047	2016	2
March 24	203	0.050	2109	7
March 25	188	0.049	2088	6
March 26	187	0.055	2330	5
March 27	191	0.055	2347	4
March 28	199	0.052	2203	—
March 29	176	0.051	2169	—
March 30	204	0.050	2126	Cyclone Betty
March 31				no survey
April 1	188	0.043	1816	
April 2	258	0.035	1493	
April 3	259	0.036	1527	
April 11	312	0.031	1331	
April 15	190	0.041	1761	
April 19	296	0.031	1323	

much larger than the over-estimates. The largest residuals (*i.e.*, ±0.2 m) occur along: (1) the beach berm, which is aligned diagonally across the centre of the grid; and (2) along the foredune toe.

By comparison, the April 2 cross-validation residuals are uniformly small across the beach grid and again the largest residuals occur along the foredune toe. The clustering of the largest residuals (*i.e.*, ±0.2 m) near the grid boundary demonstrates the importance of adequate sample density, even when the variogram model is a good descriptor of the spatial continuity of the regionalised variable. The superior performance of the April 2 model is due to its relatively smaller nugget value, which in turn reflects the less complex beach morphology at the time.

Beach Volume Changes

Table one summarises the results of the difference of means, two-tailed, t-test for observed daily changes in average (trend) residual beach elevations. The average error in daily beach elevation (95% C.I. ± 0.045 m) was equivalent to a volumetric error of 1914 m³ or about 1.0% of the average beach grid volume above −2.1-m MSL. The difference of means test showed that during the period of gradual beach accretion increases in beach volume could be detected on average every 5.8 days. After the Cyclone Betty storm of March 30–31, daily reductions in average beach elevations were detected.

Table 2. *Comparison of Gaussian variogram models fitted to complete and partial data sets, March 25 and April 2 surveys.*

No. of Profiles	Nugget (γh)	Scale (γh) Cross-shore	Scale (γh) Longshore	Range (m) Cross-shore	Range (m) Longshore
March 25					
16	0.0120	0.220	0.096	45.3	86.0
8	0.0120	0.215	0.101	40.5	88.9
4	0.0140	0.255	0.180	49.5	250.0
2	0.0005	0.133		31.4	
April 2					
16	0.0020	0.112	0.049	43.6	85.5
8	0.0018	0.118	0.058	45.7	112.2
4	0.0010	0.119	0.079	40.2	154.8
2	0.0010	0.156		42.9	

Longshore Profile Spacing

The effect of increased profile spacing on the modelled variogram parameters is presented in Table 2. The variogram models based on the full and partial data sets were similar for April 2. By comparison, the model parameters fitted to the March 25 residual elevation data diverged when the number of profiles used was less than eight. General trends in the model parameters observed with increased profile spacing included reduction in the nugget value, increased scales and ranges in the longshore axis and smaller variations in the cross-shore range (Figure 9). At least eight profiles were required to fit variogram models similar to the complete data set.

Figure 10 shows the effect of profile spacing on modelling 3D beach shape for the March 25 survey. The kriged beach surfaces based on 16 and 8 profiles are similar. Inaccuracies in modelling the beach berm are evident when the number of profiles is halved again. Despite the poor representation of beach 3D shape, estimated beach volumes based on two profiles are only 3% (March 25) and 6% (April 2) more than the kriged volumes based on sixteen profiles.

The effect of profile spacing and sample size on detection of statistically significant changes in residual elevation during the period of gradual beach accretion before Cyclone Betty is shown in Table 3. Reducing the number of profiles from 16 to 8 increased the average period required to detect changes in beach elevation from 5.8 to 7 days. It was not possible to detect changes in beach elevation when less than five profiles were used. In all cases the number of days required to reject the null hypothesis (*i.e.*, average daily beach elevations are equal) exceeded the record length (*i.e.*, March 7–30). Although the calculated t-values depend on the pooled estimation error, which reflects the sample size, the sample location is also important. This can be seen by considering two cases with pairs of profiles 1 m and 1000 m apart. The standard error about the average elevation will be less for the 1-m case than the 1000-m case because the sample variance increases with the separation distance.

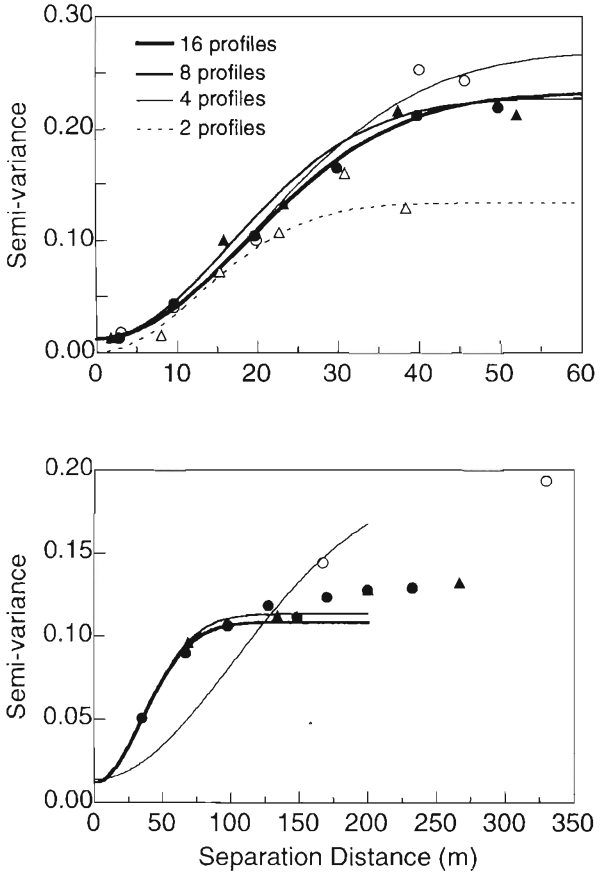

Figure 9. Effect of profile spacing on variogram models fitted to (a) cross-shore and (b) longshore experimental variograms (symbols). March 25 beach survey.

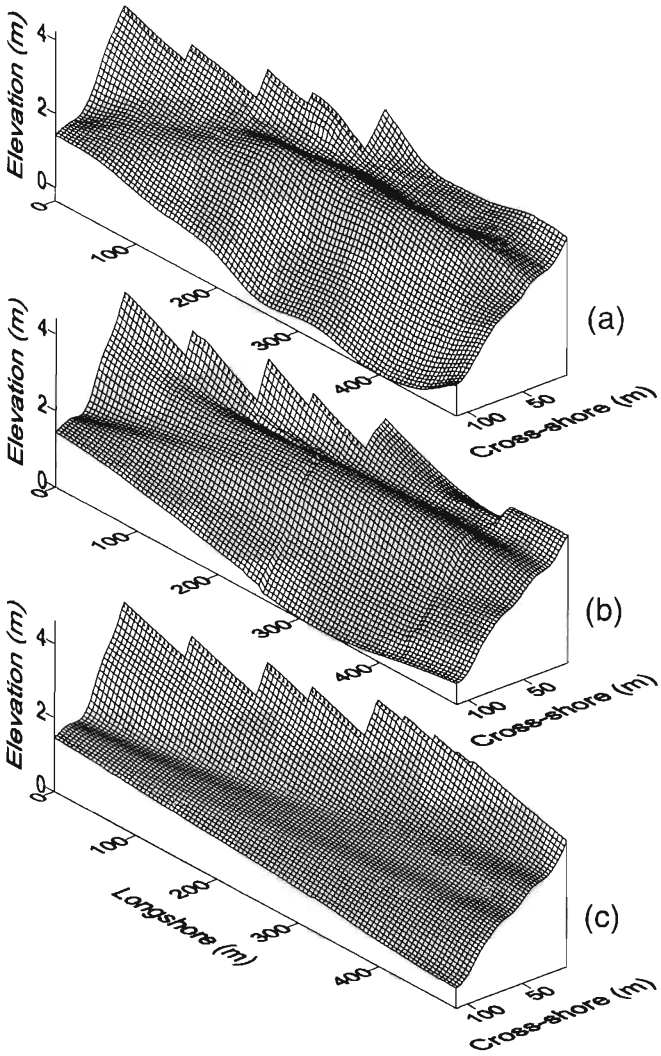

Figure 10. Kriged beach surface for March 25 based on variogram models fitted to (a) 16 or 8 profiles, (b) 4 profiles and (c) 2 profiles. The longshore profile spacings are 33, 71, 167 and 500-m respectively.

Beach Morphology and Sand Budget

Figure 11 depicts the cycle of gradual beach accretion, rapid storm erosion and subsequent post-storm recovery observed during the experiment.

The daily profile surveys began on March 7, immediately after storm erosion, with the beach depleted of sand (Figure 11a). Over the next 10 days the bar on the lower beach migrated 40 m onshore, which formed a berm at the high tide level. Landward of the berm a 0.3-m deep wash-over channel formed, which drained to the sea at the southern end of the beach (Figure 11b). Onshore sand transport under swell waves continued to build the beach berm and eventually infilled the wash-over drainage channel. By the end of March the berm had increased substantially in size, forming a 15-m wide horizontal platform on the upper beach, flanked by subtle rhythmic topography with regular 100-m longshore spacing (Figure 11c). Although the daily increases in the beach sand volume prior to Cyclone Betty were small and incremental, the cumulative effect on beach morphology was substantial. Most of the sand that accumulated on the beach was associated with berm construction (+1-m elevation change), with some of this sand supplied by erosion of the lower beach (−0.8-m elevation change) (Figure 12). Between March 7–29 the beach volume increased by 6284 m^3 and averaged 300 m^3 d^{-1} or 0.007 m^3 m^{-2} d^{-1} (Figure 13).

The Cyclone Betty storm removed 7630 m^3 of sand from the beach grid. Beach morphology immediately after Cyclone

Table 3. *Average number of days required to detect statistical differences in beach volume based on sample size.*

No. of Profiles	Profile Spacing (m)	Average Sample Size	Average No. Days
16	31	230	5.8
8	71	130	7.0
6	100	94	7.4
5	125	82	8.1
4	167	63	> record length
2	500	29	> record length

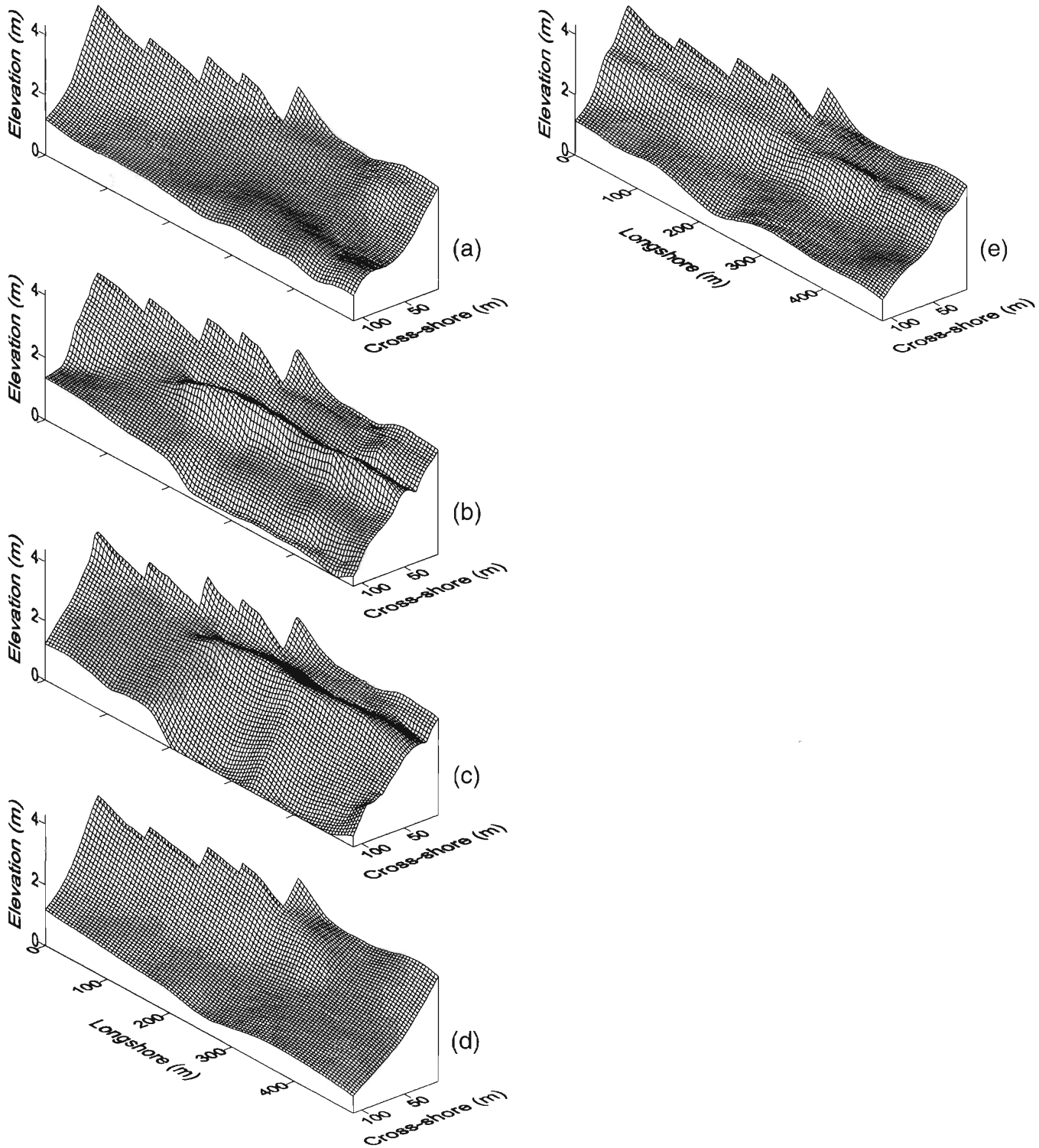

Figure 11. Changes in beach morphology during period of beach accretion: (a) March 7, (b) March 17, (c) March 30; storm erosion (d) April 1; and subsequent post-storm beach accretion (e) April 19.

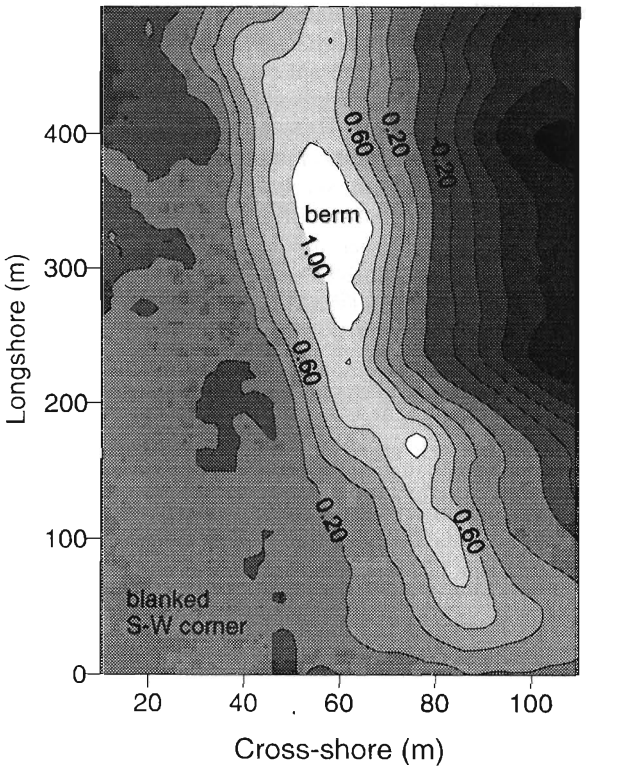

Figure 12. Contour map of beach accretion between 7–29 March under low swell waves prior to Cyclone Betty.

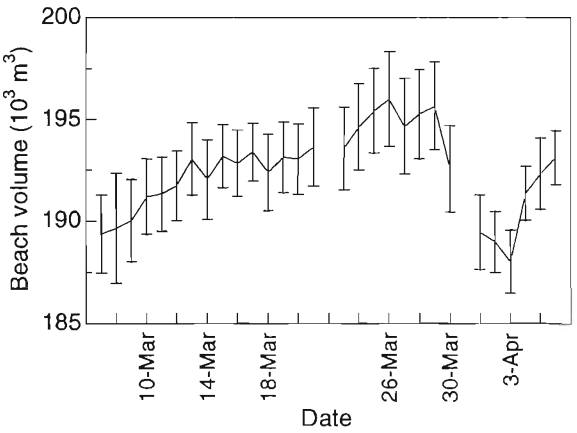

Figure 13. Changes in beach volume, March 7–April 19, 1996, with 95% confidence intervals shown.

Betty (Figure 11d) was similar to that at the beginning of the experiment. Comparison of pre- and post-storm beach surfaces shows that sand that had accumulated on the upper beach was eroded (−1-m) and a large quantity of sand (+0.8-m) was deposited on the lower beach, which filled the concavities formed by rhythmic topography (Figure 14). In the two weeks after Cyclone Betty, a high-tide berm was re-constructed (Figure 11e) with the beach sand volume increasing at a similar rate (318 m^3 d^{-1}) as before the storm.

DISCUSSION

Geostatistical Estimation

The ability to customise kriging, by modelling the semivariogram as well as explicit definition of estimation errors provided by the ordinary kriging variance and cross-validation, are defining characteristics of geostatistical estimation.

In many real-world applications, the stationarity assumption of ordinary kriging is seldom met. Data de-trending is therefore an important component of a geostatistical study, particularly since how closely the variogram model approximates the 'true' pattern of spatial continuity is conditioned by the de-trending procedure. The effect of non-stationarity on the experimental variogram was demonstrated by PHILLIPS' (1985) geostatistical study of beach profiles. However, in that study a bulldozer inadvertently 'de-trended' the beach surface and a much clearer pattern of spatial continuity emerged. In the present study, a planar de-trend of the beach elevation data was sufficient to produce stationary residuals most of the time. Onshore sand transport and berm construction prior to the storm was reflected in the emergence of a non-planar trend in cross-shore variograms at large separation distances. By fitting the variogram model to smaller lags, the effect of the higher order trend was negated. In any case, the ill-condition of the input matrices in-

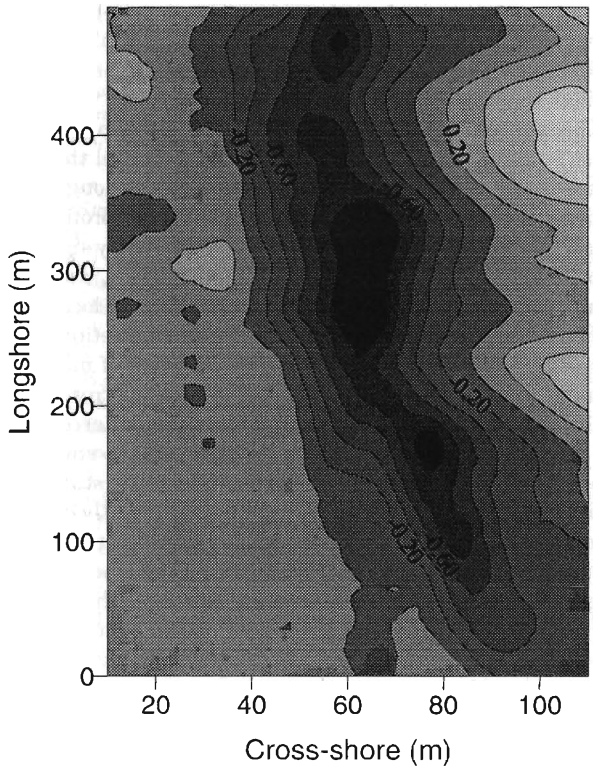

Figure 14. Contour map of beach erosion resulting from the Cyclone Betty Storm, March 29–April 3, 1996.

dicated that filtering the profile data with a higher-order trend was not justified.

UNWIN (1975b) has shown that data clustering induces ill-conditioning in the system of equations used to derive trend surface coefficients. In this study, samples are clustered in the respect that they are concentrated along shore-normal beach profiles. However, it is unusual to have regularly spaced samples and in fact this is the objective of spatial estimation. CARTER and SHANKAR's (1997) suggestion of piecewise application of linear trends to data sub-sets may overcome the inherent problem of matrix ill-condition and the need to filter polynomial trends in some applications.

In the present study, the experimental variograms of the beach elevation trend residuals displayed a very high level of spatial continuity and are similar to results obtained by PHILLIPS (1985) in his variogram study of a sandy beach. Consequently, there is very little ambiguity involved in variogram modelling and very good fits to the experimental data were obtained. By comparison, in FRENCH *et al.*'s (1995) geostatistical study of tidal marsh sedimentation, experimental variograms displayed considerable scatter, which reflected the more variable pattern of estuarine sedimentation.

The Gaussian models fitted to most of the experimental variograms are indicative of a very continuous natural phenomenon. Consequently, the proximity rather than the number of nearby samples is important to the estimation. This leads to some sampling redundancy, as clustered samples may carry no more weight than a single sample. The consistently lower variogram sill in the longshore direction is expected because the longshore grid-axis is orientated approximately with the beach contours (*i.e.,* low elevation variance). However, there is enough complexity in longshore beach shape to produce appreciable differences in the semi-variance at lags less than the range (MASON *et al.*, 1997).

The analysis of longshore profile spacing shows that at least 8 profiles were required to accurately model the experimental variogram and beach morphology. Although differences in daily beach volumes based on 16 and 2 profiles were small (*i.e.,* $\leq 6\%$), the ability to detect statistically significant short-term changes in average beach elevation, and hence beach volume, is determined by sample size and location.

The average rate of daily beach volume accretion during the experiment (0.007 $m^3\ m^{-2}\ d^{-1}$) is an order of magnitude smaller than both the average daily estimation error (0.04 $m^3\ m^{-2}\ d^{-1}$) but similar to the survey measurement error (0.004 $m^3\ m^{-2}\ d^{-1}$), without accounting for errors due to small-scale topography. Therefore, it is not surprising that statistically significant daily increases could not be consistently detected. The average point elevation error (0.045 m) is still likely to be much smaller than the errors induced by small-scale topography. BRAMPTON (1990) has argued that a height accuracy of 0.1 m on sand beaches is reasonable given the 'noise' level caused by rapid spatial and temporal changes in beach topography (MASON *et al.,* 1997).

Implications for Beach Monitoring

Mangawhai is an important source of construction sand for Auckland (pop. ~1.1 million), which is New Zealand's largest city. Nearshore sand-mining, in water depths of 3–8 m, has occurred in the 25-km Mangawhai-Pakiri embayment since the 1940's and at least 2.73×10^6 m^3 of sand has been extracted since 1966. The present rate of sand extraction is 110×10^3 $m^3\ yr^{-1}$, and there are questions regarding the sustainability of this mining (HESP and HILTON, 1996; HILTON, 1989). Environmental impact assessments of the sand extraction have in the past largely relied on determining long-term trends in shoreline stability. This work has been based on the analysis of 8 beach profiles that have been surveyed on average every 6 months since 1978. The profiles were established shortly after a series of storms that severely eroded many east coast beaches, including Mangawhai Beach (HESP and HILTON, 1996).

Separate analyses of the beach profile record have reached opposite conclusions: (a) the profiles indicate a long term trend of net beach accretion; and (b) the profiles show an episodic cycle of storm erosion and subsequent beach accretion, along an otherwise stable or eroding sandy coast. The former interpretation has been used to argue that nearshore sand extraction has had no adverse effect on the coastal sand system (HESP and HILTON, 1996).

The present study highlights the inadequacies of using individual beach profiles to make inferences about 3D beach morphology and sand budgets. Accurate representations of beach–shoreface morphology are required for numerical modelling of waves and sediment transport. Considerable variations in longshore beach morphology do occur over relatively short spatial and temporal scales. On beaches that display rhythmic topography this variability is exacerbated. In the present experiment, 8 profiles were required to accurately model beach morphology and to obtain beach sand volumes with acceptable estimation errors. The geostatistical analyses attempted with 2 profiles produced quite misleading results because naive assumptions about the spatial continuity of the beach surface were necessary.

An alternative approach is to monitor the behaviour of a beach segment and use geostatistical tools, such as variogram modelling and ordinary kriging, to accurately model beach morphology and sand budget. The sampling strategy will depend on the spatial structure of the beach surface and the objectives of a particular study. For example, monitoring the performance of a beach re-nourishment project may require more intensive and frequent sampling than monitoring long-term beach trends. The present study also shows that how often a beach can be monitored to detect changes will be constrained by the estimation error. These questions of how often and how intensively to sample can be answered by a pilot geostatistical study. Variogram modelling can be used to determine the spatial structure of the beach surface and cross-validation used as a guide to model performance. This information can then be used to customise the monitoring requirements for a particular beach.

Statistical analysis of the Mangawhai data set has shown that detecting short-term changes in a beach sand budget is more difficult during phases of beach accretion in comparison to the obvious effects of storm erosion. The average time interval between surveys to detect statistically significant changes in beach volume will also depend on the sampling

strategy because the volume estimation error is a function of the location and number of samples. The sampling strategy will ultimately depend on the objectives of a particular study. Geostatistics provides the tools to make informed decisions about monitoring beach behaviour.

CONCLUSIONS

The present study has a number of implications for monitoring short-term changes in beach morphology and sand budgets. Firstly, data de-trending is an important aspect of any geostatistical study to satisfy the stationarity assumption. Also, how closely the variogram model approximates the 'true' pattern of spatial continuity is conditioned by the trend model. In this study, a planar trend model was sufficient to produce stationary elevation data most of the time. The ill-condition of the input matrices precluded fitting higher order trends. Secondly, experimental variograms of beach elevation data display a high level of spatial continuity. Consequently there is little ambiguity involved in variogram modelling and in most cases good fits to the experimental data will be obtained. Thirdly, it is difficult to detect short-term changes in beach volume during periods of accretion, in comparison to periods of storm erosion, because apparent volumetric changes are an order of magnitude lower than the estimation error and of a similar order as the measurement error. In this study it was possible to detect significant increases in beach volume on average every 5.8 days during 3-weeks of gradual sand accretion by swell waves. Lastly, an alternative approach to beach monitoring using individual profiles is to monitor a beach segment. Geostatistical tools can be used to model beach morphology and to obtain accurate estimates of beach volume. The sampling strategy will depend on the complexity of beach morphology and the objectives of a particular study.

ACKNOWLEDGEMENTS

The author thanks Keith Smith and Ron Ovenden (NIWA Hamilton) for providing beach profile data. I am grateful to Murray Hicks and Glenn Carter (NIWA Christchurch), Evan Englund (US EPA National Exposure Research Laboratory) and Terry Healy (Coastal Marine Group, University of Waikato) for helpful discussions and reviews of the manuscript. The study was funded by the New Zealand Foundation for Research, Science and Technology under contract number CO1511.

LITERATURE CITED

BRAMPTON, A.H., 1990. *Coastline Monitoring.* Report IT 345. Hydraulics Research, Wallingford, U.K., 14p.

CARTER, G.S. and SHANKAR, U., 1997. Creating rectangular bathymetry grids for environmental numerical modelling of gravel-bed rivers. *Applied Mathematical Modelling,* 21, 699–708.

DAVIS, J.C., 1986. *Statistics and data analysis in geology, 2nd edition.* New York: Wiley, 646p.

CHAPRA, S.C. and CANALE, R.P., 1998. *Numerical Methods for Engineers: with programming and software applications, 3rd Edition.* Boston: McGraw-Hill, 924p.

CLARK, I., 1979. *Practical Geostatistics.* London: Applied Science Publishers Ltd, 129p.

CRESSIE, N., 1990. The origins of kriging. *Mathematical Geology,* 22(3), 239–252.

DOLAN, R.; FENSTER, M.S., and HOLME, S.J., 1992. Spatial analysis of shoreline recession and accretion. *Journal of Coastal Research,* 8(2), 263–285.

EMERY, K.O., 1961. A simple method for measuring beach profiles. *Limnology and Oceanography,* 6, 90–93.

ENGLUND, E. and SPARKS, A., 1991. *Geostatistical Environmental Assessment Software GEO-EAS 1.2.1 Users Guide.* Las Vegas, Nevada, Environmental Monitoring Systems Laboratory, United States Environmental Protection Agency, 130p.

FRENCH, J.R.; SPENCER, T.; MURRAY, A.L., and ARNOLD, N.S., 1995. Geostatistical analysis of sediment deposition in two small tidal wetlands, Norfolk, U.K. *Journal of Coastal Research,* 11(2), 308–321.

GOLDEN SOFTWARE INC., 1995. *SURFER® for windows, version 6 user's guide,* Golden, Colorado, 450p.

GOODMAN, A., 1983. Data clusters and trend surfaces. *Monash Publications in Geography No. 29.* Department of Geography, Monash University, Melbourne, 57p.

GROSSKOPF, W.G. and KRAUS, N.C., 1994. Guidelines for surveying beach nourishment projects. *Shore and Beach,* 62(2), 9–16.

HESP, P. and HILTON, M.J., 1996. Nearshore-surfzone system limits and the impacts of sand extraction. *Journal of Coastal Research,* 12(3), 726–747.

HICKS, D.M. and GREEN, M.O., 1997. The 'fall-speed parameter' as an index of cross-shore sand transport: verification from measurements on the shoreface. *Proceeding 13th Australasian Coastal and Ocean Engineering Conference and 6th Australasian Port and Harbour Conference.* (Centre for Advanced Engineering, New Zealand), Pp. 1089–1094.

HILTON, M.J., 1989. Management of the New Zealand coastal sand mining industry: some implications of a geomorphic study of the Pakiri coastal sand body. *New Zealand Geographer,* 45(1), 14–25.

HILTON, M.J., 1995. Sediment facies of an embayed coastal sand body, Pakiri, New Zealand. *Journal of Coastal Research,* 11(2), 529–547.

ISAAKS, E.H. and SRIVASTAVA, R.H., 1989. *Applied Geostatistics.* New York: Oxford University Press, 557p.

MASON, D.C.; DAVENPORT, I.J., and FLATHER, R.A., 1997. Interpolation of an intertidal digital elevation model from heighted shorelines: a case study in the Western Wash. *Estuarine, Coastal and Shelf Science,* 45, 599–612.

MATHERON, G., 1963. Principles of geostatistics. *Economic Geology,* 58, 1246–1266.

PANNATIER, Y., 1996. Variowin: Software for spatial data analysis in 2D. *Statistics and Computing Series.* New York: Springer-Verlag, 91p.

PHILLIPS, J.D., 1985. Estimation of optimal beach profile sample intervals. *Journal of Coastal Research,* 1(2), 187–191.

POSA, D., 1988. Conditioning of the stationary kriging matrices for some well-known covariance models. *Mathematical Geology,* 21(7), 755–765.

SMITH, R.K.; LATIMER, G.J.; SWALES, A.; RUTHERFORD, J.C.; BUDD, R.G.; OVENDEN, R., and HAMBLING, J., 1997. Nearshore profile and bedform measurement using an enhanced sea sled survey technique. *Shore and Beach,* 65(4), 15–22.

SWALES, A.; HICKS, D.M., and SMITH, R.K., 1999. Shoreface bedforms and cross-shore sand fluxes measured using an enhanced sea sled. *Proceeding Coastal Sediments '99,* (American Society Civil Engineers), Pp. 1034–1049.

THE MATHWORKS INC., 1995. *MATLAB® High-performance numeric computation and visualisation software,* Mass., U.S.A., 548p.

UNWIN, D.J., 1975. An introduction to trend surface analysis. *Concepts and Techniques in Modern Geography.* Geo Abstracts Ltd, University of East Anglia, Norwich, 40p.

UNWIN, D.J., 1975b. Numerical errors in a familiar technique: a case study of polynomial trend surface analysis. *Geographical Analysis,* 7, 197–203.

WRIGHT, L.D. and SHORT, A.D., 1984. Morphodynamic variability of surf zones and beaches: a synthesis. *Marine Geology,* 56, 93–118.